Structure–Activity Relationship Studies of Retro-1 Analogues against Shiga Toxin

Hajer Abdelkafi, Aurélien Michau, Valérie Pons, Flora Ngadjeua, Alexandra Clerget, Lilia Ait Ouarab, David-Alexandre Buisson, David Montoir, Lucie Caramelle, Daniel Gillet, et al.

HAL Id: hal-03320788

https://hal.inrae.fr/hal-03320788

Submitted on 19 Dec 2023

Structure-activity relationship studies of Retro-1 analogues against Shiga toxin

Hajer Abdelkafi[†], Aurélien Michau[‡], Valérie Pons[†], Flora Ngadjeua[‡], Alexandra Clerget[‡], Lilia Ait Ouarab[†], David-Alexandre Buisson[†], Lucie Caramelle[‡], Daniel Gillet[‡,], Julien Barbier[‡], and Jean-Christophe Cintrat[†,*]*

[†]Université Paris-Saclay, CEA, INRAE, Médicaments et Technologies pour la Santé (MTS), SCBM, 91191 Gif-sur-Yvette, France
[‡]Université Paris-Saclay, CEA, INRAE, Médicaments et Technologies pour la Santé (MTS), SIMoS, 91191 Gif-sur-Yvette, France

ABSTRACT

The Retro-1 molecule was identified in a high-throughput screening as an inhibitor of ricin and Shiga toxins by diminishing their intracellular trafficking *via* the retrograde route, from early endosomes to the Golgi apparatus. In order to improve the activity of Retro-1, a SAR study was undertaken yielding an analog that possesses roughly 70-fold better EC_{50} against Shiga toxin cytotoxicity measured in a cell protein synthesis assay.

Retro-1
EC_{50} (Stx) : 6 µM

(*S*)-Retro-1.1
EC_{50} (Stx) : 90 nM
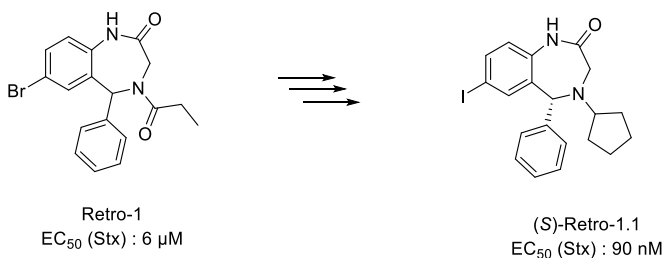
INTRODUCTION

Shiga toxins (Stx) are a family of structurally and functionally similar protein toxins produced by *Shigella dysenteriae* and some serogroups of *Escherichia coli*.[1] Gram-negative bacteria producing Stx are pathogenic and responsible for a number of human foodborne diseases such as bloody diarrhea and the hemolytic uremic syndrome (HUS), the most feared complication of the infection defined by acute renal failure, thrombocytopenia and microangiopathic hemolytic anemia.[2]

Stx belong to the group of AB_5 toxins and consist of a catalytically active A-subunit (StxA) and a binding pentameric B-subunit (StxB). After binding of StxB to the globotriaosylceramide (Gb3) receptor at the cell surface, Stx is endocytosed and traffics through endosomes to the endoplasmic reticulum (ER) by the retrograde pathway.[3] Once in ER, StxA translocates to the cytosol where it arrests protein biosynthesis of host cells by enzymatically inactivating ribosomes.

Hitherto, no specific therapies are available to treat Stx intoxication. At the hospital, management of HUS is based on general supportive care, and early dialysis for acute renal failure. Plasma exchange has been explored without indication of its efficacy.[4, 5] Yet, the massive outbreak of Stx-producing *E. coli* in Germany in 2011 allowed assessment of new drugs, such as the humanized monoclonal antibody Eculizumab directed against the complement protein C5 and approved for the treatment of the genetic related disorder atypical HUS (aHUS). However, a retrospective study concluded to an absence of benefit for Eculizumab-treated HUS patients.[4]

Blocking of intracellular retrograde trafficking of Stx can be a viable strategy to arrest the intracellular action of the toxin as demonstrated with different chemical compounds.[6-9] Identified by HTS, Retro-1 selectively blocked Stx retrograde trafficking at the early endosome-trans Golgi network (TGN) interface, hence protecting exposed cells from the cytotoxic action of Stx.[8] Unlike different small molecules that inhibit intracellular Stx transport, Retro-1 did not perturb cellular

morphology nor did it affect other trafficking pathways. Here, we report on the development of a related compound Retro-1.1 with a similar mode of action and conferring an improved protection efficacy against Stx on human cells.

RESULTS AND DISCUSSION

Synthesis of Retro-1. The synthesis of compound **6**, Retro-1, was achieved starting from the commercially available 2-amino, 5-bromo benzophenone **1** (Scheme 1) in 39% yield over 4 steps. First, regioselective bromination was performed with NBS with complete conversion. Acetylation with bromo acetyl bromide was immediately followed by cyclisation with ammonia to yield the benzodiazepine **4** in 66 % yield over two steps. Then, reduction of the imino moiety with NaBH$_3$CN offered the two enantiomers of benzodiazepine **5** that were treated with propionyl chloride to get Retro-1 as a mixture of two enantiomers. In addition, racemic Retro-1 was obtained as a 1:1 mixture of conformers as detected by ^{1}H and ^{13}C NMR.[10] High temperature NMR allowed us to obtain coalescence of the two conformers signals (see supplementary materials).

Scheme 1 here

Evaluation of benzodiazepine drugs and derivatives. We first started to evaluate the biological activities of few commercially available (some are marketed drugs) related analogs of Retro-1 along with different other structural analogs we synthesized (Figure 1). The latter were obtained via the synthetic route depicted in Scheme 1 starting either from commercially available aminobenzophenones or that were synthesized in house (by a Friedel-Craft reaction between the desired aniline and the corresponding benzonitrile). All tested molecules are depicted in Figure 1.

3

Figure 1 here

All of these compounds were inactive which strongly suggests that a benzodiazepine scaffold and not a benzodiazepinone one is mandatory.

Modification of N4. We then checked the impact of the N4 amide substitution by introducing small variations around the propionyl group.

Table 1 here

Unfortunately, the four amide analogs we synthesized proved inactive (Table 1, compounds **22**, **24**, **25**) or less active than the parent Retro-1 (Table 1, compound **23**) in Stx protection assays. It has to be stated again that Retro-1 (vide infra) but also analogs presented in Table 1 (compounds **22**-**25**) give rise to conformers assumedly due to the presence of the tertiary amide. We therefore decided to synthesize a reduced analog of Retro-1 *id est* compound **26**. Compound **26** was indeed the best analog showing a slightly better protection compared to Retro-1 (6 µM to 4 µM, Table 1). This reduced analog not only allowed to get an active compound but also to get rid of conformers hence simplifying the analysis. This propylated compound was therefore a good starting point for a more extensive SAR studies. Based on this N-propyl analog we then investigated the impact of the N1 amide substitution (Table 2).

Substitution at N1. None of the analogs we synthesized in this series proved active against Shiga toxin either with aliphatic substituents (Table 2, compound **27**), allylic or benzylic (compounds **32** and **33**) or aromatic/heteroaromatic (compounds **28**-**31**). These results suggest that the NH bond is crucial for bioactivity and may be involved in H bonding with the target(s) or may point to a small hydrophilic cavity.

Table 2 here

Modification of the aromatic rings. Facing these rather disappointing results we then decided to evaluate the impact of the BZD phenyl ring substitution. This later was functionalized either by a palladium catalyzed cross-coupling, taking advantage of the bromine at C7, or by the use of initially functionalized 2-aminobenzophenones (Table 3).

Table 3 here

Based on palladium coupling reactions, various aromatic (compounds **34**, **35**, **38**), heteroaromatic (compounds **36**, **37**) were synthesized but were completely inactive. 9-bromo or 8-methoxy derivatives of compound **29** were also obtained (compounds **39**, **40**) but with no efficiency to protect cells against Stx. The substitution of the bromide at C7 by a chloride, iodide or azide maintained the protection of the cells against Stx (compounds **41**, **42**, **43**).

Substitution at C5. Because of the difficulty of late stage modifications, we decided to obtain some modified benzodiazepines at C5 from different 2-amino, 5-bromobenzophenone analogs. These latter were either commercially available (Table 4, compounds **45**, **46**, **48**) or obtained by Friedel-Craft reaction between the 5-bromoaniline and the corresponding benzonitrile (compound **44**).

Table 4 here

Compound **47** was obtained via a directed palladium iodination reaction previously developed in our group.[11] Except for 2-monofluorinated analogue (compound **46**) and 2,4-difluorinated analogues (compound **48**), all compounds tested proved less potent than compound **29**. Despite the fact that the fluoride atom is slightly larger than hydrogen atom little change to the steric bulk of the molecule is usually seen. The biggest changes in bioactivity are usually due to large electronegativity difference between these two atoms (besides to higher lipophilicity of fluoride), but here there seems to be no influence of this parameter on bioactivity against Stx even if a better cell membrane permeation cannot be ruled out.

Modification at the N4 secondary amine. In a final round of the SAR, based on the previous experience with the reduction of the propionyl substituent (see Table 2) we studied more extensively the effect of substitution on the secondary amine.

The introduction of substituents was possible thanks either to reductive amination or nucleophilic substitution from compound **5**.

Table 5 here

Numerous analogues were synthesized and tested. First, compounds bearing an indole ring were obtained but were less active than Retro-1 (compound **49**). Then pyridine substituents were introduced (4-substituted, compound **50** or 3-substituted pyridine, compound **51**) but both compounds did not show improved efficiency. The naphthyl derivative **52** was completely inactive. Closely related structure, the quinoline moiety **53** showed lower activity compared to Retro-1. Then few small heterocyclic substituents such as thiophenyl (compounds **54, 55**), or furyl (compounds **56**, **57**) were synthesized and screened but without any improvement. Phenyl substituent was introduced either with a one (compound **58**) or a three methylene linker (compound **59**) but with complete loss of activity. Then many aliphatic substituents (compounds **60-70**) were introduced and we obtained more potent inhibitors especially with acyclic or cyclic derivatives (compounds **66, 68, 69**). It has to be noticed that more sterically demanding ramified aliphatic chains (compounds 6**3, 67**) or substituted aliphatic rings (compound **70**) gave lower bioactivity. The most promising candidates in this series were cyclopentyl derivatives (compounds **66, 68, 69**). Finally functionalized aliphatic chains were inactive (compounds **71-73**), or less active (compound **74**).

Halide effect. Having the best analog in hand (compound **66**), we focused our attention towards the effect of the bromide since we already experienced a change in bioactivity with different halogens at C7 (see Table 4, compounds **41**, **42**). Therefore, we synthesized analogs containing respectively no halide (**75**), fluoride (**76**), chloride (**77**) and iodide (**78**). Iodinated analog (compound **78**) afforded an improved EC_{50} value of 300 nM and suggests that a putative X-bond with electron-rich groups present in the target(s) might be involved to account for this ranking of halogenated derivatives (Figure 2).[12, 13]

Figure 2 here

Since compound **78** was the best analogue of Retro-1 synthesized during this SAR studies we decided to name it Retro-1.1.

Separation of enantiomers and attribution of configuration and biological activities.
A chiral phase separation of the enantiomers of Retro-1.1 was carried out on a ChiralPak IA HPLC which allowed us to obtain two enantiomers Retro-1.1.a and Retro-1.1.b.

Figure 3 here

In order to determine the absolute configuration of each enantiomer, we decided to take advantage of the enantiomers of Retro-1 assignment that was previously performed thanks to X-ray crystallography:[10]

Scheme 2 here

Then HeLa cells were challenged against Stx in presence of each enantiomer of Retro-1.1 (Figure 4). (*S*)-enantiomer of Retro-1.1 proved to be the eutomer as was already experienced with Retro-1.[10]

Figure 4 here

To prove that the mode of action of Retro-1.1 obtained herein prevents the deleterious effect of Stx by blocking its intracellular trafficking through the retrograde pathway as reported for Retro-1, we examined the subcellular distribution of the fluorescent-labeled Stx. These experiments

definitely showed that Shiga toxin is not able to reach the Golgi apparatus in the presence of (*S*)-Retro-1.1 whereas (*R*)-Retro-1.1 appeared unable to block Stx trafficking inside cells (Figure 5).

CONCLUSION

Based on SAR studies, we were able to obtain benzodiazepinones with enhanced potency to protect cells against Shiga toxin compared to the parent molecule Retro-1. This SAR shows that a halogen atom at C7 is mandatory. The most active compound, (*S*)-Retro-1.1 now affords an EC_{50} of 90 nM corresponding to a 70-fold improvement compared to the parent Retro-1. We also showed that this compound blocks the retrograde trafficking of Shiga toxin. Experiments are in progress to decipher the mode of action of this compound and to identify its cellular target(s). As Retro-1 blocks retrograde trafficking similarly to Retro-2, it would be worth testing optimized Retro-1 compounds against various pathogens in particular viruses such as poxvirus,[14] cytomegalovirus[15] and enterovirus 71[16] for which Retro-2 derivatives proved efficient.

EXPERIMENTAL SECTION

Synthesis

All chemicals and solvents used in the syntheses were reagent grade and were used without additional purification. THF and CH_2Cl_2 were distilled respectively from sodium/benzophenone ketyl and calcium hydride before use. Glassware was flame-dried under vacuum and cooled under nitrogen to room temperature. All reactions were performed under dry nitrogen gas and monitored by thin-layer chromatography (TLC). TLC was performed with precoated TLC silica gel 60 F254,

and organic compounds were visualized by UV light (254 nm), iodine vapor, phosphomolybdic acid [10% (w/v) in ethanol] staining with heating.

The large-scale purification was performed on a CombiFlash with a UV-vis detector with RediSep columns. The samples were adsorbed on Celite or silica and loaded into solid load cartridges. An ethyl acetate/cyclohexane or methanol/methylene chloride gradient was employed. Fractions were collected based on UV detection at 254 nm.

HPLC-MS analysis and purification were performed using a Waters system (2525 binary gradient module, in-line degasser, 2767 sample manager, 2996 Photodiode Array Detector) with a binary gradient solvent delivery system. This system was coupled with a Waters Micromass ZQ system with a ZQ2000 quadrupole analyzer. The ionization was performed by electrospray and the other parameters were as follows: source temperature 120 °C, cone voltage 20 V, and continuous sample injection at 0.3 mL/min flow rate. Mass spectra were recorded in both positive and negative ion mode in the m/z 100-2,000 range and treated with the Mass Lynx 4.1 software.

The eluent was a gradient of (99.9% water / 0.1% HCOOH) and (99.9% MeCN / 0.1% HCOOH) or (99.9% water / 0.1% HCOOH) and (99.9% MeOH / 0.1% HCOOH). Each compound was applied to a 100 x 4.6 mm (5 µm) WATERS XBridge C18 column equilibrated with H_2O/MeCN or H_2O/MeOH 95:5.

Gradient A: Samples were eluted by increasing MeOH to 100% (25 min) then 100% (5 min).

Gradient B: Samples were eluted by increasing MeOH to 90% (24 min), then 100% (1 min) and stay at 100% (5 min).

Gradient C: Samples were eluted by increasing MeOH to 80% (24 min), then 100% (1 min) and stay at 100% (5 min).

Gradient D: Samples were eluted by increasing MeCN to 100% (25 min) then 100% (1 min).

Gradient E: Samples were eluted by increasing MeCN to 90% (24 min), then 100% (1 min) and stay at 100% (5 min).

Gradient F: Samples were eluted by increasing MeCN to 80% (24 min), then 100% (1 min) and stay at 100% (5 min).

Gradient G: Samples were eluted by increasing MeCN to 60% (24 min), then 100% (1 min) and stay at 100% (5 min).

HPLC (Chiral) analyses were performed on a system equipped with a binary gradient solvent delivery system (LC-20AB, Shimadzu), a SIL-20A autosampler (Shimadzu), and a photodiode array detector (SPD-20A, Shimadzu).

The purity of the compounds was assessed by UPLC/UV/MS (ESI+ and ESI-) using a WATERS Acquity system equipped with a BEH XBridge C18 column (1.7 µM, 2.1*50 at 40 °C) and purity is usually ≥95% from of one the analysis detection mode. Elution conditions are as follows :

Solvant :   A : H_2O+1/1000 HCO_2H, B : ACN+1/1000 HCO_2H

T0	0.4 mL/min	95%A 5%B
T3min	0.4 mL/min	0%A 100%B
T3.1min	0.6 mL/min	0%A 100%B
T4min	0.6 mL/min	0%A 100%B

NMR experiments were performed on a Bruker Avance 400 Ultrashield spectrometer. ^{1}H-NMR and ^{13}C spectra were recorded at room temperature at 400 MHz and 100 MHz respectively, samples were dissolved in DMSO-D6 at a concentration of approximately 5 mM. The DMSO singlet signal was set up at 2.50 ppm. Chemical shifts are given in ppm and the coupling constants in Hz. Spectral data are consistent with assigned structures.

High-resolution mass spectrometry (HRMS) was recorded on ESI/TOF LCP premier XE mass spectrometer (Waters) using flow injection analysis mode.

Chemicals for *in vitro* experiments

The following products were purchased from the indicated commercial sources: [^{14}C]-leucine (Perkin-Elmer), Shiga-like toxin 2 (Stx, List Biological Laboratories, Inc.), DMSO (Sigma), fetal bovine serum (Sigma), glutamine, pyruvate, non-essential amino acids and antibiotics solutions (Gibco). Alexa-488-StxB was prepared as previously described.[17]

Intoxication assays

HeLa cells were maintained at 37 °C under 5% CO_2 in DMEM (Dulbecco's modified Eagle's medium, Invitrogen), supplemented with 10% fetal bovine serum, 4.5 g/L glucose, 100U/mL penicillin, 100 µg/mL streptomycin, 4 mM glutamine, 5 mM pyruvate. The cells were plated at a density of 50,000 cells per well in 96-well Cytostar-T[TM] scintillating microplates (Perkin-Elmer) with scintillator incorporated into the polystyrene plastic. After incubation with either 30 µM or various concentration of compounds (or 0.1 % DMSO) for 4 hours at 37 °C, cells were challenged with increasing doses of Stx in the continued presence of compounds. After incubation for 20 hours, the medium was removed and replaced with DMEM without leucine (Eurobio) containing

10% fetal bovine serum, 2 mM L-glutamine, 0.1 mM non-essential amino acids, 1% Penicillin/Streptomycin supplemented by 0.5 µCi/mL [^{14}C]-leucine. The cells were grown for an additional 6 hours at 37 °C in an atmosphere of 5% CO_2 and 95% air. Protein biosynthesis was then determined by measuring the incorporation of radiolabelled leucine into cells using a Wallac 1450 MicroBeta liquid scintillation counter (Perkin Elmer).

The mean percentage of protein biosynthesis was determined and normalized from duplicate wells. Data were fitted with Prism v5 software (Graphpad Inc., San Diego, CA) to obtain the 50% inhibitory toxin concentration (IC_{50}) *i.e.* the concentration of toxin that is required to kill 50% of cells. IC_{50} values and protection factor R ($R = IC_{50}$ drug/IC_{50} DMSO) were determined by the software's nonlinear regression "dose-response EC_{50} shift equation". The goodness of fit for Stx alone (carrier) or with drug was assessed by r^2 and confidence intervals. The percentage of cell protection was calculated for each compound after determination of R value (Rdrug) and compared to the R value of Retro-1 (Rref):

$$\% \, protection = \frac{Rdrug - 1}{Rref - 1} \times 100$$

All compounds were tested at 30 µM and Retro-1 compound equals to a 100% protection at 30 µM.

Determination of EC_{50} values

For compounds that displayed a percentage of protection equal or superior to 100%, the EC_{50} represents the concentration giving 50% of its full inhibitory effect against Stx. EC_{50} was used to compare compounds efficacy because it is more precise than R values and associated % protection. This is due to the fact that R values may fluctuate between cell experiments from different 96-

wells plates corresponding to compounds tested on different days. In contrast EC_{50} value for a single compound is calculated from experimental data obtained on a single 96-well plate. Cell assays were performed with various concentrations of the inhibitor. For each concentration, a percentage of protection was determined from R values calculated with Prism software with Rmax corresponding to the higher value of R of the series:

$$\% \, protection = \frac{R - 1}{Rmax - 1} \times 100$$

Drug concentration was plotted against the corresponding percentage of protection of cells and the 50% efficacy concentration (EC_{50}) was calculated by non-linear regression using the Prism software package.

Fluorescent staining

For fluorescence experiments, compound-treated HeLa cells were pre-incubated for 1 hour in the continued presence of compounds (1 µM). Compound-treated cells were then incubated with Alexa 488-StxB (0.1 µg/mL) for 30 min on ice, followed by 45 min at 37°C in the continued presence of compounds (1 µM). After washing, cells were then fixed with a solution of paraformaldehyde (4%, 5 min), labeled with phalloidin-Atto-550 (1/1000, Sigma) for actin staining and DAPI (1 µg/mL, Sigma) dissolved in the mounting medium for nuclei staining. Samples were imaged on an inversed SP8x confocal microscope (Leica) using a 63x oil immersion objective, NA 1.4. Maximum projections of optical Z slices are shown.

FIGURES
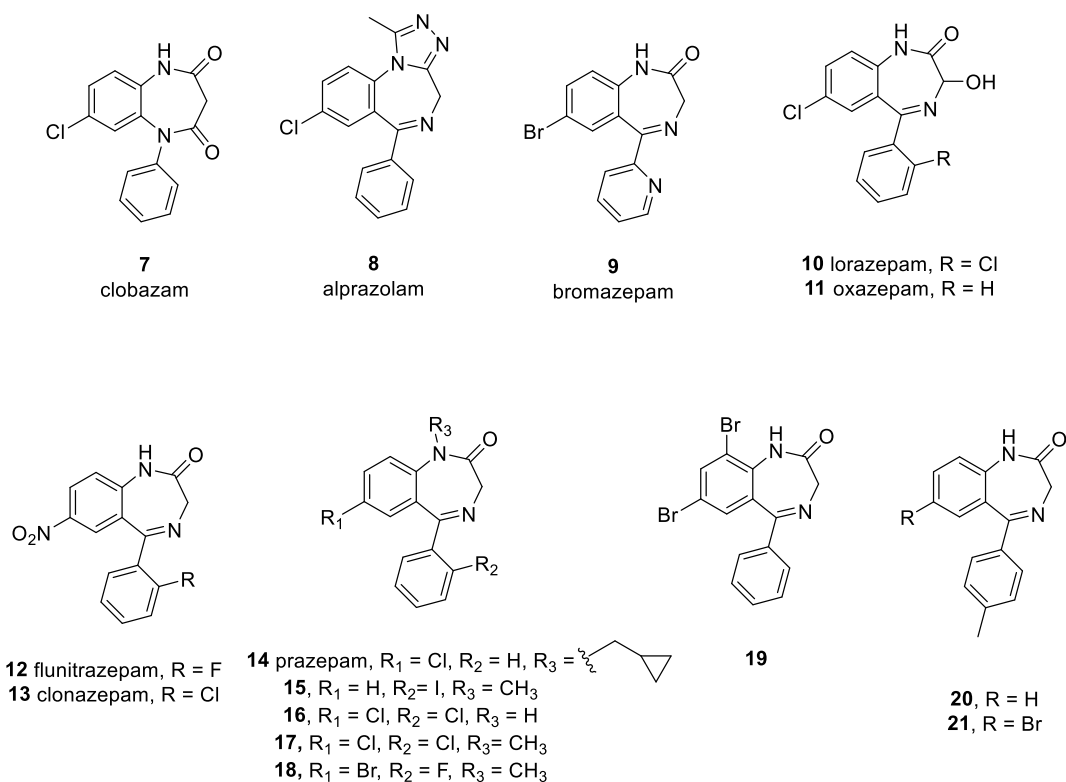
Figure 1. Initial screening of commercially available benzodiazepinones and miscellaneous derivatives
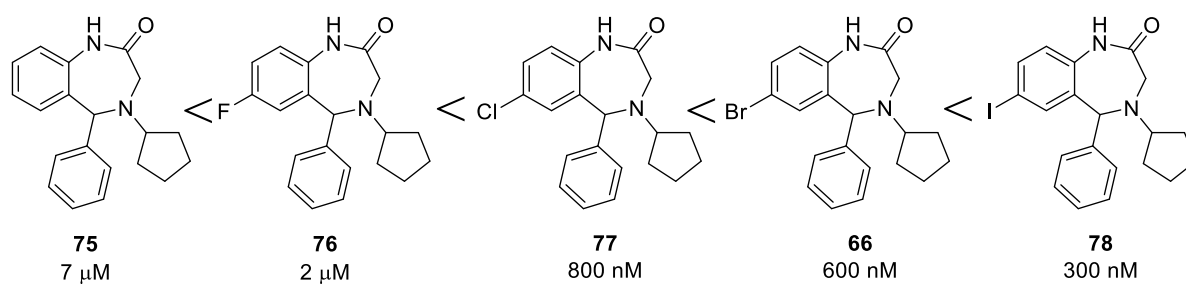
Figure 2. Effect of halogen at C7 on the bioactivity against Shiga toxin
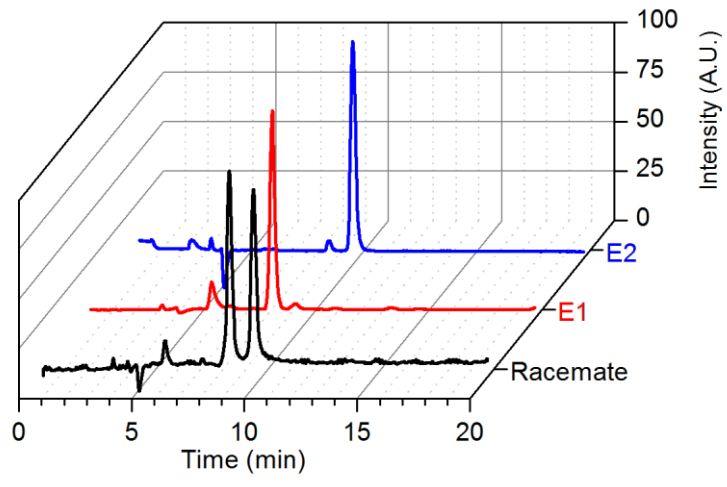
Figure 3. Chiral HPLC of Retro-1.1 racemate and enantiomers
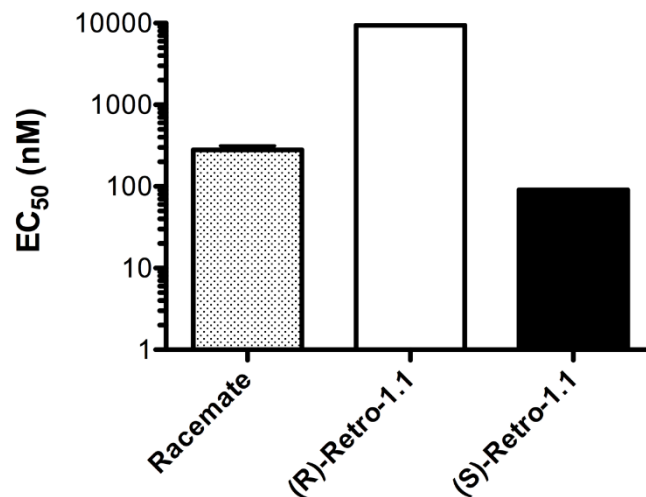
Figure 4. Evaluation of protective activity towards Stx cytotoxicity of each enantiomer of Retro-1.1. HeLa cells were incubated for 4 hours with racemic Retro-1.1 (grey), (*R*)-Retro-1.1 (white)**,** or (*S*)-Retro-1.1 (black) before the addition of Stx for 20 hr. Media was removed and replaced with DMEM containing [^{14}C]-leucine at 0.5 μCi/mL for 7 hr before counting. Each data point represents the mean of duplicate ± SD of two independent experiments.
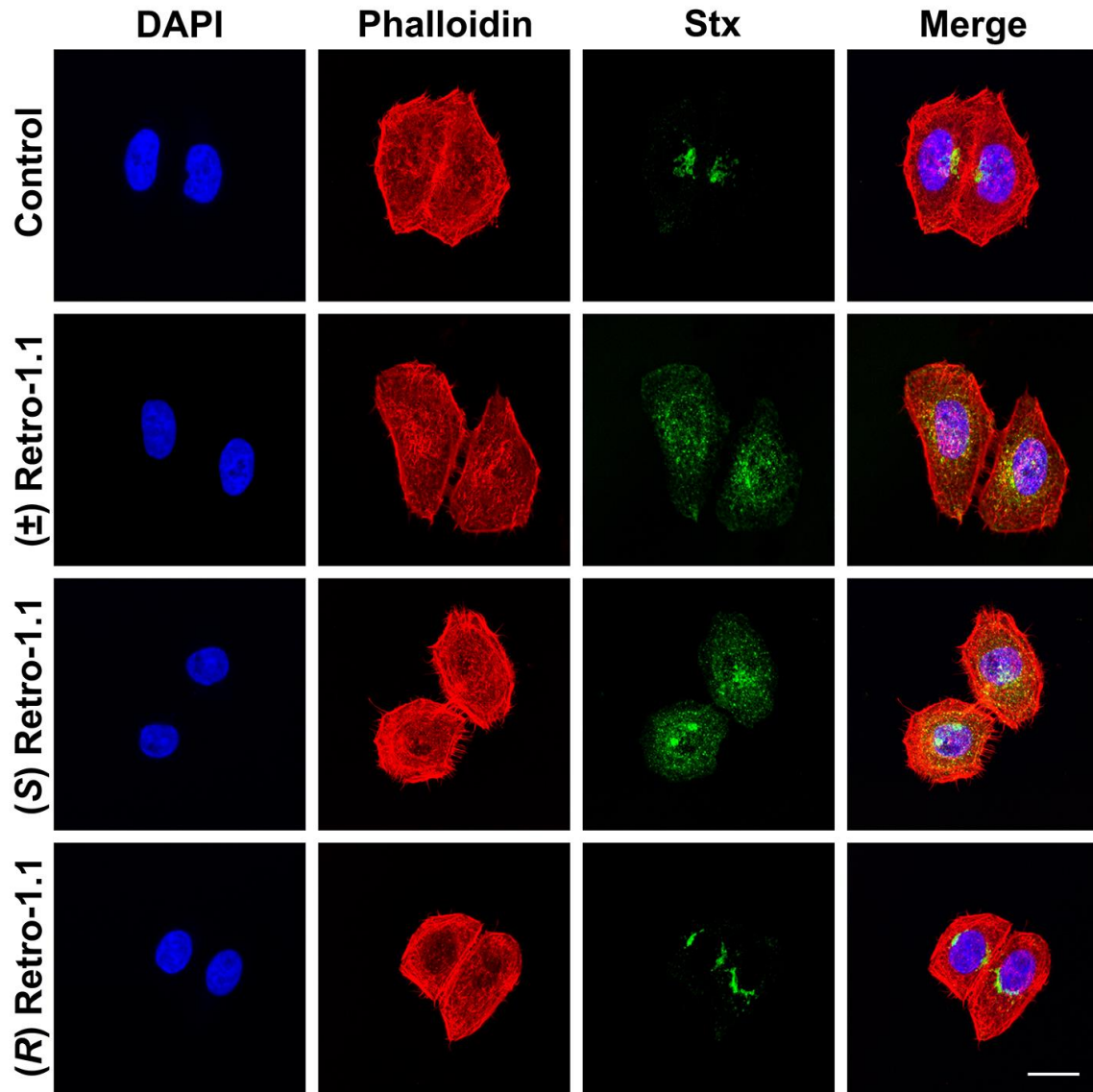
Figure 5. (±)-Retro-1.1 and (*S*)-Retro-1.1 block the retrograde transport of Shiga toxin. Cells were pretreated for 1 hr with (±)-Retro-1.1 (upper panel), (*S*)-Retro-1.1 (middle panel) or (*R*)-Retro-1.1 (lower panel) at 1 µM before addition of Alexa488-labeled StxB (0.1 µg/mL, green). Cells were fixed with 4% PFA, and labeled with phalloidin-Atto-550 (red) and DAPI (blue) for actin and nuclei staining respectively. Scale bar, 20 µm.

Scheme 1. Synthetic route to Retro-1
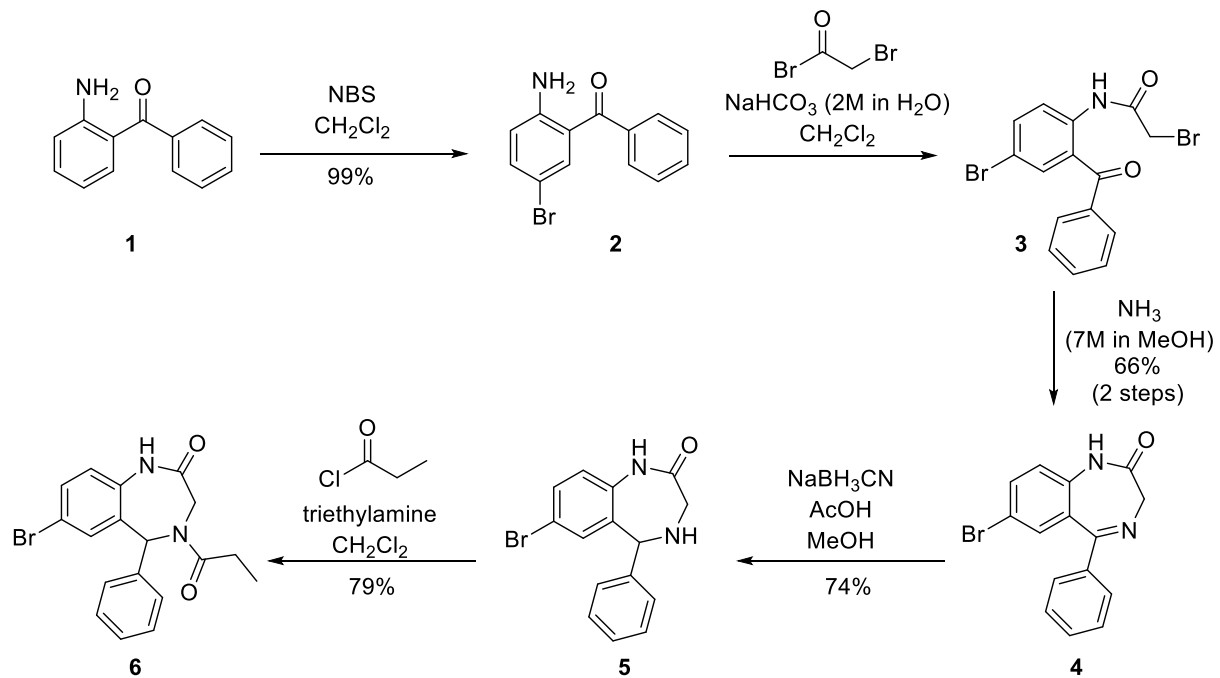
Scheme 2. Strategy to determine the absolute configurations of compounds **5** and **78** (Retro-1.1)

Step 1: We synthesized the two enantiomers of Retro-1 from the separated enantiomers of **5** which allowed us retrospectively to identify (*S*)-**5** and (*R*)-**5**.
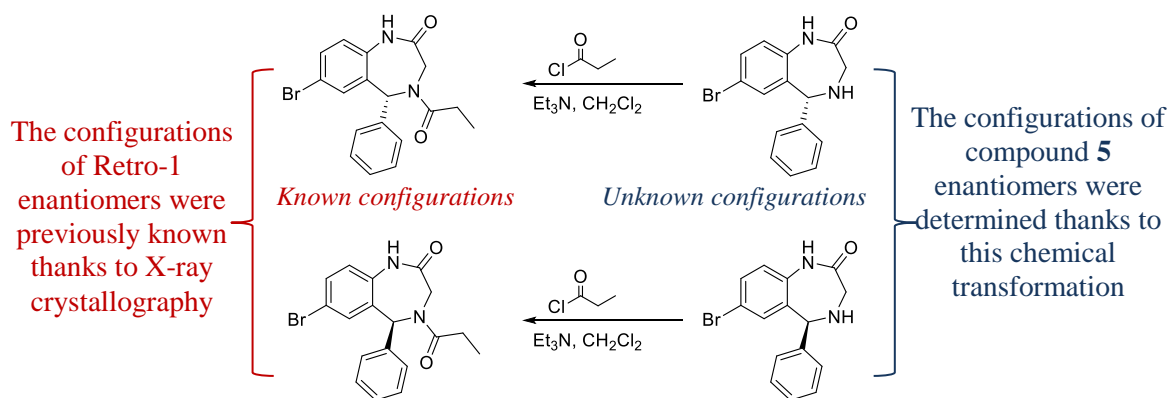
Step 2: With the assignment of compound **5** enantiomers in hand we decided to perform a two steps chemical modification, knowing that no inversion of configuration could occur during these transformations, which allowed us to obtain a HPLC profile of (*S*)-Retro-1.1 and (*R*)-Retro-1.1.
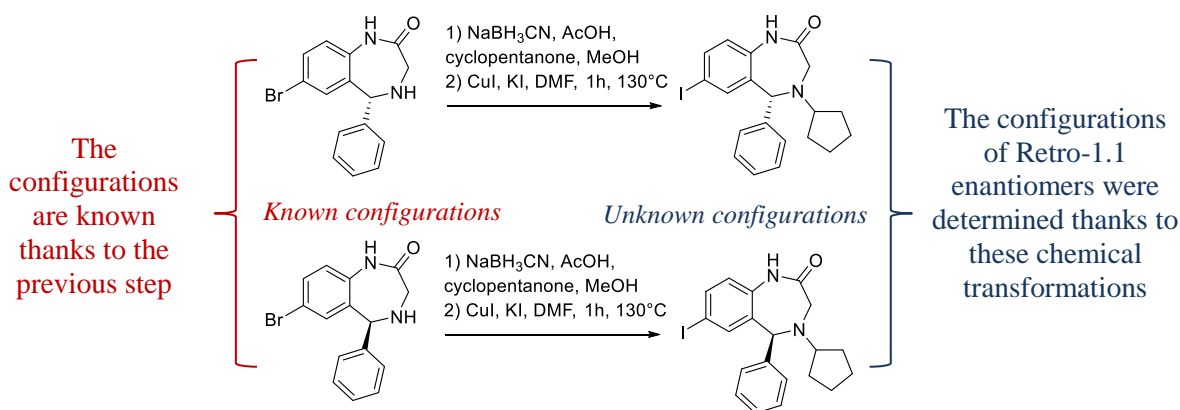
TABLES.

Table 1. Preliminary evaluation of the substitution at N4
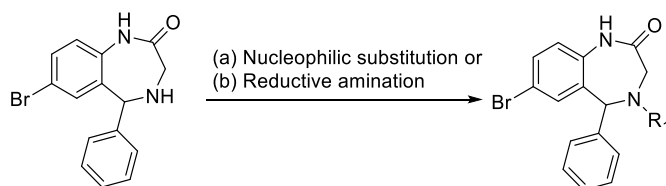
compound	R₁	Yield (%)	Protection (%)	EC₅₀ (μM)
22		50	inactive	n.d.
23		78	80.2	11.2
24		84	inactive	n.d.
25		83	inactive	n.d.
26		91	>100	4.0

Table 2. Modification on the N1 amide
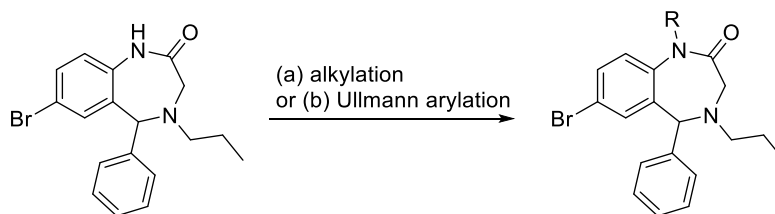
Compound	R	Yield (%)	Protection (%)	EC$_{50}$ (μM)
27	Me→	48	inactive	n.d.
28		50	inactive	n.d.
29	F$_3$C	41	inactive	n.d.
30		52	inactive	n.d.
31		37	inactive	n.d.
32		81	inactive	n.d.
33		70	inactive	n.d.

Table 3. Evaluation of the substitution at the phenyl benzodiazepine ring
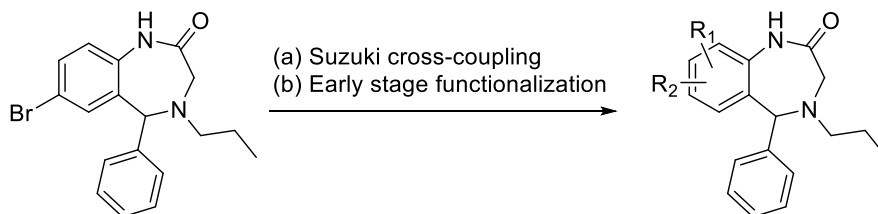
Compound	Structure	Yield (%)	Protection (%)	EC$_{50}$ (µM)
34		93	inactive	n.d.
35		20	inactive	n.d.
36		56	inactive	n.d.
37		70	inactive	n.d.
38		55	inactive	n.d.
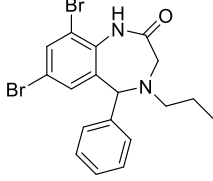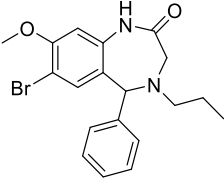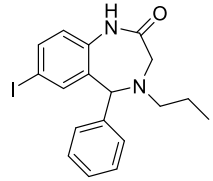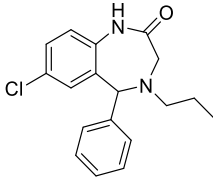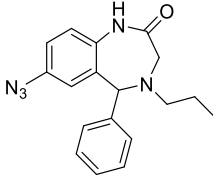
39		72	inactive	n.d.
40		44	30.7	n.d.
41		54	>100	4.0
42		99	>100	13.6
43		56	>100	11
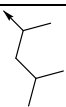
Table 4. Evaluation of substitution at C5
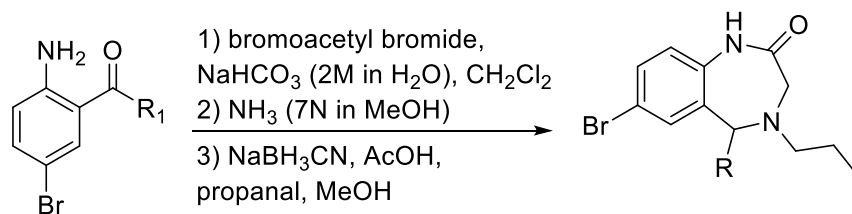
Compound	R	Yield (%)	Protection (%)	EC$_{50}$ (µM)
44	4-pyridyl	66	14.4	n.d.
45	4-methylphenyl	56	inactive	n.d.
46	2-fluorophenyl	62	>100	3.9
47	2-iodophenyl	71	59.6	n.d.
48	2,4-difluorophenyl	21	>100	12.8

Table 5. Structure-activity relationship of compounds modified at N4

a) Reductive amination or
b) Nucleophilic substitution
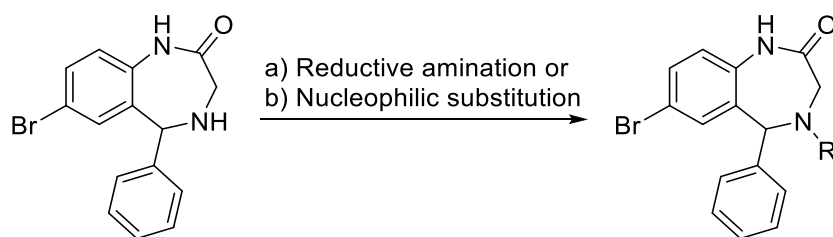
| Compound	R	Yield (%)	Protection (%)	EC$_{50}$ (μM)
49		50	20.6	n.d.
50		79	5.3	n.d.
51		91	38.8	n.d.
52		85	inactive	n.d.
53		74	29.9	n.d.
54		86	58.2	n.d.
55		88	12.2	n.d.
56		92	2.9	n.d.
57		88	Inactive	n.d.
58		95	Inactive	n.d.
59		78	Inactive	n.d.

5	H	74	Inactive	n.d.
60	Me	90	Inactive	n.d.
61		23	85.8	8.8
62		85	29.5	n.d.
63		62	Inactive	n.d.
64		24	>100	4.7
65		27	>100	5.2
66		64	>100	0.6
67		46	Inactive	n.d.
68		57	>100	1.3
69		63	>100	3.9
70		72	Inactive	n.d.
71		47	Inactive	n.d.
72		100	Inactive	n.d.
73		55	Inactive	n.d.
74		38	>100	6.5

27

ASSOCIATED CONTENT

Supporting Information.

The following files are available free of charge.

Synthetic procedures (PDF)

Supplementary information on NMR spectra (PDF)

AUTHOR INFORMATION

Corresponding Author

* JCC Tel: + 33 1 69 08 21 07. Fax: + 33 1 69 08 79 91. Email: jean-christophe.cintrat@cea.fr

* DG Tel: + 33 1 69 08 76 46. Fax: + 33 1 69 08 90 71. Email: daniel.gillet@cea.fr

Author Contributions

The manuscript was written through contributions of all authors. All authors have given approval to the final version of the manuscript.

ABBREVIATIONS

Stx, Shiga toxin; HUS, Hemolytic uremic syndrome; Gb3, Globotriaosylceramide; ER, endoplasmic reticulum; TGN, trans Golgi network; NBS, N-bromosuccinimide; HRMS, High resolution mass spectrometry.

REFERENCES

(1)   Bergan, J.; Dyve Lingelem, A. B.; Simm, R.; Skotland, T.; Sandvig, K. Shiga toxins. *Toxicon* **2012,** 60, 1085-107.

(2)   Tarr, P. I.; Gordon, C. A.; Chandler, W. L. Shiga-toxin-producing Escherichia coli and haemolytic uraemic syndrome. *Lancet* **2005,** 365, 1073-86.

(3)   Johannes, L.; Romer, W. Shiga toxins--from cell biology to biomedical applications. *Nat Rev Microbiol* **2010,** 8, 105-16.

(4)   Menne, J.; Nitschke, M.; Stingele, R.; Abu-Tair, M.; Beneke, J.; Bramstedt, J.; Bremer, J. P.; Brunkhorst, R.; Busch, V.; Dengler, R.; Deuschl, G.; Fellermann, K.; Fickenscher, H.; Gerigk, C.; Goettsche, A.; Greeve, J.; Hafer, C.; Hagenmuller, F.; Haller, H.; Herget-Rosenthal, S.;

Hertenstein, B.; Hofmann, C.; Lang, M.; Kielstein, J. T.; Klostermeier, U. C.; Knobloch, J.; Kuehbacher, M.; Kunzendorf, U.; Lehnert, H.; Manns, M. P.; Menne, T. F.; Meyer, T. N.; Michael, C.; Munte, T.; Neumann-Grutzeck, C.; Nuernberger, J.; Pavenstaedt, H.; Ramazan, L.; Renders, L.; Repenthin, J.; Ries, W.; Rohr, A.; Rump, L. C.; Samuelsson, O.; Sayk, F.; Schmidt, B. M.; Schnatter, S.; Schocklmann, H.; Schreiber, S.; von Seydewitz, C. U.; Steinhoff, J.; Stracke, S.; Suerbaum, S.; van de Loo, A.; Vischedyk, M.; Weissenborn, K.; Wellhoner, P.; Wiesner, M.; Zeissig, S.; Buning, J.; Schiffer, M.; Kuehbacher, T.; consortium, E.-H. Validation of treatment strategies for enterohaemorrhagic Escherichia coli O104:H4 induced haemolytic uraemic syndrome: case-control study. *BMJ* **2012,** 345, e4565.

(5)   Tarr, P. I.; Sadler, J. E.; Chandler, W. L.; George, J. N.; Tsai, H. M. Should all adult patients with diarrhoea-associated HUS receive plasma exchange? *Lancet* **2012,** 379, 516; author reply 516-7.

(6)   Barbier, J.; Bouclier, C.; Johannes, L.; Gillet, D. Inhibitors of the cellular trafficking of ricin. *Toxins (Basel)* **2012,** 4, 15-27.

(7)   Saenz, J. B.; Doggett, T. A.; Haslam, D. B. Identification and characterization of small molecules that inhibit intracellular toxin transport. *Infect Immun* **2007,** 75, 4552-61.

(8)   Stechmann, B.; Bai, S. K.; Gobbo, E.; Lopez, R.; Merer, G.; Pinchard, S.; Panigai, L.; Tenza, D.; Raposo, G.; Beaumelle, B.; Sauvaire, D.; Gillet, D.; Johannes, L.; Barbier, J. Inhibition of retrograde transport protects mice from lethal ricin challenge. *Cell* **2010,** 141, 231-42.

(9)   Wahome, P. G.; Bai, Y.; Neal, L. M.; Robertus, J. D.; Mantis, N. J. Identification of small-molecule inhibitors of ricin and shiga toxin using a cell-based high-throughput screen. *Toxicon* **2010,** 56, 313-23.

(10)   Abdelkafi, H.; Michau, A.; Clerget, A.; Buisson, D. A.; Johannes, L.; Gillet, D.; Barbier, J.; Cintrat, J. C. Synthesis, Chiral Separation, Absolute Configuration Assignment, and Biological Activity of Enantiomers of Retro-1 as Potent Inhibitors of Shiga Toxin. *ChemMedChem* **2015,** 10, 1153-6.

(11)   Abdelkafi, H.; Cintrat, J. C. Regioselective Halogenation of 1,4-Benzodiazepinones via CH Activation. *Sci Rep* **2015,** 5, 12131.

(12)   Lu, Y.; Shi, T.; Wang, Y.; Yang, H.; Yan, X.; Luo, X.; Jiang, H.; Zhu, W. Halogen bonding--a novel interaction for rational drug design? *J Med Chem* **2009,** 52, 2854-62.

(13)   Sirimulla, S.; Bailey, J. B.; Vegesna, R.; Narayan, M. Halogen interactions in protein-ligand complexes: implications of halogen bonding for rational drug design. *J Chem Inf Model* **2013,** 53, 2781-91.

(14)   Harrison K.; Haga I. R.; Pechenick Jowers T.; Jasim S.; Cintrat J.-C.; Gillet D.; Schmitt-John T.; Digard P.; Beard P. M. Vaccinia virus uses retromer independent cellular retrograde transport pathways to facilitate the wrapping of intracellular mature virions during virus morphogenesis. *J Virol* **2016**, 90, 10120-32.

(15)   Desai D.; Lauver M.; Ostman A.; Cruz L.; Ferguson K.; Jin G.; Roper B.; Brosius D.; Lukacher A.; Amin S.; Buchkovich N. Inhibition of diverse opportunistic viruses by structurally optimized retrograde trafficking inhibitors. *Bioorg Med Chem* **2019**, 27, 1795-1803.

(16)   Dai W.; Wu Y.; Bi J.; Lu X.; Hou A.; Zhou Y.; Sun B.; Kong W.; Barbier J.; Cintrat J.-C.; Gao F.; Gillet D.; Su W.; Jiang C. Antiviral effects of Retro-2(cycl) and Retro-2.1 against Enterovirus 71 *in vitro* and *in vivo*. *Antiviral Res* **2017**, 14, 311-321.

(17)   Amessou, M.; Popoff, V.; Yelamos, B.; Saint-Pol, A.; Johannes, L. Measuring retrograde transport to the trans-Golgi network. *Curr Protoc Cell Biol* **2006,** Chapter 15, Unit 15 10.

Table of Contents graphic

Optimized benzodiazepinones against Shiga toxins

Retro-1
EC$_{50}$ (Stx) : 6 µM

(S)-Retro-1.1
EC$_{50}$ (Stx) : 90 nM